Potential dual targeting of an *Arabidopsis* archaebacterial-like histidyl-tRNA synthetase to mitochondria and chloroplasts[1]

Kinya Akashi, Olivier Grandjean, Ian Small*

Station de Génétique et Amélioration des Plantes, INRA, Route de St-Cyr, 78026 Versailles Cedex, France

Received 20 March 1998; revised version received 8 June 1998

Abstract A cDNA clone encoding a histidyl-tRNA synthetase (HisRS) was characterized from *Arabidopsis thaliana*. The deduced amino acid sequence (AtHRS1) is surprisingly more similar to HisRSs from archaebacteria than those from eukaryotes and prokaryotes. AtHRS1 has an N-terminal extension with features characteristic of mitochondrial and chloroplast transit peptides. Transient expression assays in tobacco protoplasts clearly demonstrated efficient targeting of a fusion peptide consisting of the first 71 amino acids of AtHRS1 joined to jellyfish green fluorescent protein (GFP) to both mitochondria and chloroplasts. These observations suggest that the AtHisRS1 cDNA encodes both mitochondrial and chloroplast histidyl-tRNA synthetases.

Key words: Histidyl-tRNA synthetase; Mitochondrial protein import; Chloroplast transit peptide; GFP; Confocal microscopy; *Arabidopsis thaliana*

1. Introduction

Aminoacyl-tRNA synthetases (aaRSs) are a family of structurally diverse enzymes which play a crucial role in translation of genetic information by catalyzing the covalent addition of one of the 20 amino acids to their cognate tRNAs. Based on the presence of conserved sequence motifs, the aaRSs are classified into two groups (class I and II) each containing ten members [1,2]. This classification highlights the two different designs of the active site, and suggests two different evolutionary origins of the aaRS gene family. Moreover, sequence divergence during the course of evolution has generated considerable structural differences among prokaryotic, eukaryotic and archaebacterial aaRSs [3]. For example, the isoleucyl-tRNA synthetase family can be subdivided into two types present in eukaryotes/archaea and prokaryotes respectively, on the basis of presence/absence of a zinc-binding Cys-4 cluster at the C-terminus [4]. In the case of glycyl-tRNA synthetases, sequence comparison reveals no particular sequence similarity between eukaryotic/archaea and prokaryotic enzymes [5], although both types of enzymes are class II aaRSs. In some cases, such divergence results in an inability to cross-aminoacylate isoacceptor tRNAs from other species. For example, mammalian and *E. coli* glycyl-tRNA synthetases do not cross-aminoacylate their respective glycine tRNAs [5]. These taxonomic barriers are good examples of co-evolution of the aaRSs and their cognate tRNA sequences [3].

In plant cells, the protein synthesis apparatus exists in three different subcellular compartments (cytosol, mitochondria, and chloroplasts), thus full sets of aaRSs are needed within each compartment. Biochemical evidence has shown that most chloroplast and cytosolic aaRSs only charge tRNAs from the same compartment [6], suggesting that each set of aaRSs is essentially encoded by different genes. However, this might not be the case for plant mitochondrial aaRSs, because tRNAs with three different genetic origins (native mitochondrial tRNAs, chloroplast-like tRNAs, and nuclear-encoded imported tRNAs) are integrated into the mitochondrial translation system [7]. This complex situation should be reflected by the characteristics of the corresponding aaRSs, all of which are encoded by the nuclear genome and targeted to the organelle. Alanyl-tRNA synthetase (AlaRS) from *Arabidopsis* offers a good example, where a single gene encodes for both cytosolic and mitochondrial AlaRSs [8]. In this case, alternative transcription starts and translational start codons produce two polypeptides of different length at their N-terminus. The shorter protein encodes cytosolic AlaRS, the longer one is targeted to mitochondria. Dual targeting of the same AlaRS to the cytosol and mitochondria was half-expected, because both enzymes must recognize the same cytosolic-type tRNA due to the import of nuclear-encoded $tRNA^{Ala}$ into mitochondria [9].

However, knowledge of plant aaRSs remains quite limited, and little is known about aaRSs which recognize chloroplast-like mitochondrial tRNAs. To gain more information about the structure and localization of plant aaRSs, we have examined histidyl-tRNA synthetases (HisRS) from *Arabidopsis*, where the mitochondrial genome encodes a chloroplast-like $tRNA^{His}$ [10]. Biochemical data [6] have previously suggested that the chloroplast HisRS can charge both cytosolic and chloroplast tRNAs, whereas the cytosolic HisRS can only charge cytosolic $tRNA^{His}$.

2. Materials and methods

Except where stated otherwise, standard molecular biological techniques were performed using the protocols described by Ausubel et al. [11]. Full details of the cloning procedures are available on request. Oligonucleotides were purchased from Genosys (Cambridge, UK). Sequencing was performed with fluorophore-labelled primers in a semi-automated sequencing system (model 373A; Applied Biosystems).

2.1. Southern blot analysis

Total DNA of greenhouse-grown *Arabidopsis* plants was prepared as described previously [8]. Two μg of genomic DNA was digested with appropriate restriction enzymes, separated on a 0.7% agarose gel, and transferred to Hybond-N^+ nylon membrane (Amersham International, Little Chalfont, UK). Radioactive DNA probes were prepared using the Oligolabelling Kit (Pharmacia Biotech., Sweden) with α-^{32}P dCTP (Amersham), using a gel-purified 1.1-kb *Pst*I-*Xho*I fragment of

*Corresponding author. Fax: +33 1 30 83 33 19.
E-mail: small@versailles.inra.fr

[1]EMBL/Genbank/DDBJ accession no: AF020715.

PII: S0014-5793(98)00717-0

the AtHRS1 cDNA clone or a 0.5-kb *Sal*I-*Not*I fragment of the EST clone T43519 as templates. Prehybridization and hybridization were carried out at 42°C in 50% formamide, 6×SSPE, 5×Denhardt's solution, 0.5% SDS, 100 μg/ml denatured salmon sperm DNA. The hybridized filter was then washed twice for 2 min in 2×SSC, 0.1% SDS at room temperature, once for 1 h at 51°C in 1×SSC, 0.1% SDS, and once for 30 min at 51°C or 65°C in 0.1×SSC, 0.1% SDS. Autoradiography was carried out at −80°C using REFLECTION (Dupont) X-ray film and intensifying screens.

2.2. Construction of GFP fusions

The targeting sequences corresponding to the first 71, 68, and 20 amino acids of AtHRS1, *Arabidopsis* RecA, and yeast CoxIV, respectively, were PCR-amplified from cloned genes or cDNA or *Arabidopsis* genomic DNA using pairs of primers as follows; AtHRS: 5′-CACTCCATGGTCGACCCACGCGTCC-3′, 5′-CCTTCCATGGGATTGACATCGATCTTCTT-3′; RecA: 5′-AGAACCATGGATTCACAGCTAGTCTT-3′, 5′-GCGCCCATGGTTCTGTCATCGAATTCAG-3′; CoxIV: 5′-AGCACCATGGTTTCACTACGTCAATCTA-3′, 5′-TTCACCATGGGTTTTTGCTGAAGCAG-3′.

Amplified fragments were digested with *Nco*I and cloned in-frame into an *Nco*I site of the GFP expression vector pCK GFP S65C [12]. The AtHRS-GFP plasmid was further modified by oligonucleotide-mediated in vitro mutagenesis to remove its 5′-UTR sequence. The sequences of the resulting plasmids, termed AtHRS-GFP, CoxIV-GFP, and RecA-GFP were checked by sequencing, and it was confirmed that all three fusion constructs had exactly the same 5′-UTR sequences followed by the start codons of the respective targeting sequences, fused to the GFP coding region.

2.3. Transformation of tobacco protoplasts

Tobacco mesophyll protoplasts were prepared from young leaves of *Nicotiana tabacum* (cv. Xanthi, doubled haploid line XHFD8) as described previously [13]. Protoplasts were electroporated with 100 μg of the respective plasmid DNAs and incubated in the dark for 24 h before confocal microscope analysis.

2.4. GFP and MitoTracker Red visualization

Protoplasts were examined with a Leica TCS-NT confocal laser scanning microscope with an argon/krypton laser (Omnichrome, Chino, CA, USA) and a SP510 short pass filter for excitation. A reflect short pass filter (RSP580) was used to separate the emission beam in two. GFP fluorescence was collected through a long pass filter (LP515) and chloroplast autofluorescence through a second long pass filter (LP590). Slow scan (220 lines per second) images (1024×1024 pixels) were generated using a 40×/1.00–0.50 PL FLUOTAR objective.

In some experiments, MitoTracker Red CMXRos (Molecular Probes Europe, Leiden, The Netherlands) was used to stain mitochondria. The dye was added to 0.5 μM final concentration to protoplasts in 0.5 M mannitol, 5 mM KCl, 200 μM MOPS-KOH, pH 7.2 for 15–30 min. MitoTracker Red fluorescence was collected using a band pass filter (BP568) for excitation and a long pass filter (LP590) for emission.

2.5. Sequence analysis

Sequence alignments and pairwise comparisons of sequences were performed using the PILEUP and BESTFIT programs from the Wisconsin Package Version 9.1, Genetics Computer Group (GCG), Madison, WI, USA. For phylogenetic analyses, amino acid sequences from motif 1 to motif 3 of HisRSs or the nucleotide sequences of $tRNA^{His}$ were first aligned by PILEUP. Replicates were generated by SEQBOOT and used for parsimony methods (PROTPARS or DNAPARS), maximum likelihood methods (PROTML or DNAML) and distance matrix methods (DNADIST or PROTDIST followed by NEIGHBOR) in PHYLIP (J. Felsenstein, University of Washington, Seattle, WA, USA). Bootstrap percentage values were calculated by CONSENSE in PHYLIP.

3. Results

3.1. A novel archaebacterial-like HisRS from Arabidopsis

Two distinct types of *Arabidopsis* cDNAs with deduced amino acid sequences similar to those of known HisRSs from other organisms have been reported as expressed sequence tags (ESTs) [14]. One of them (Genbank accession

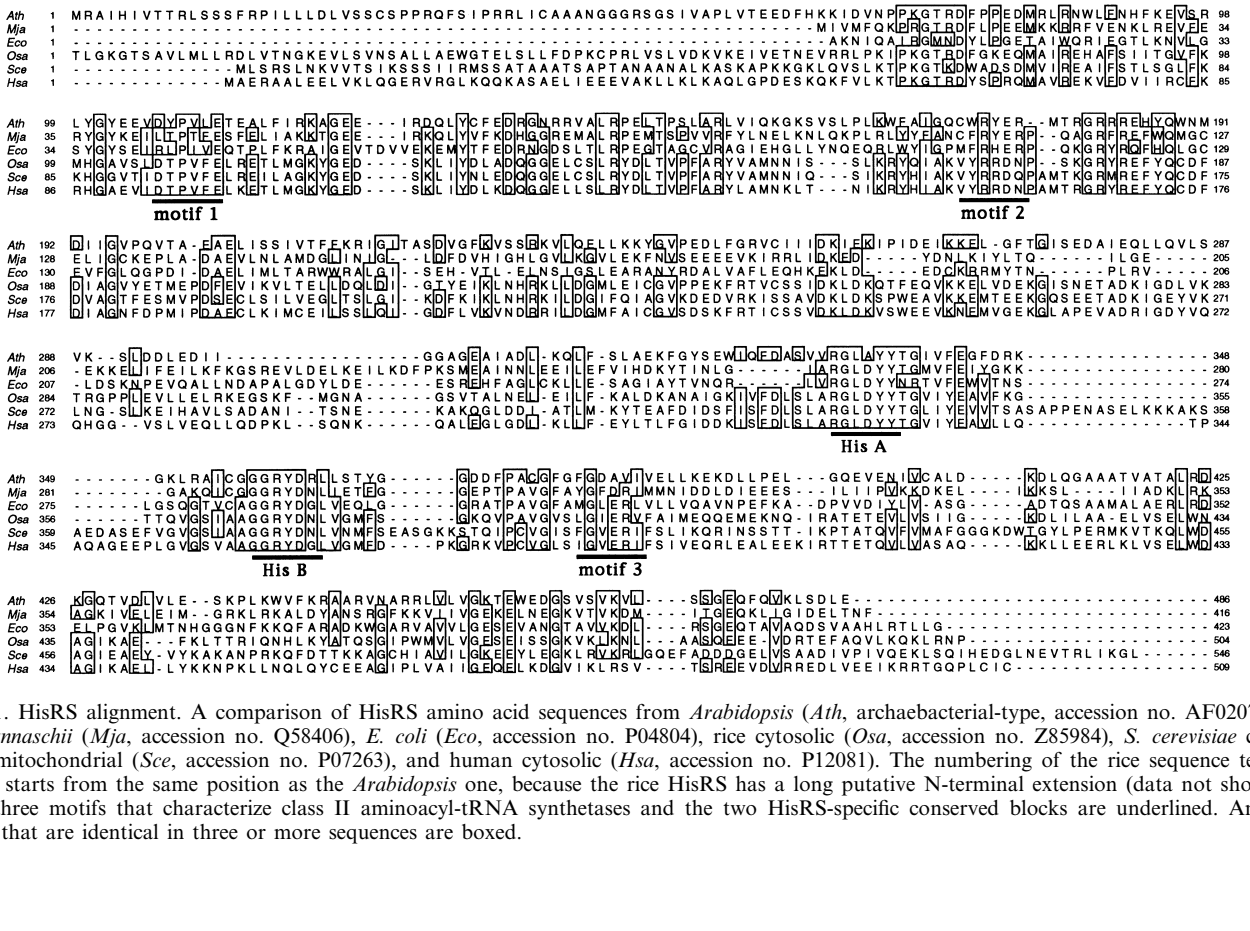

Fig. 1. HisRS alignment. A comparison of HisRS amino acid sequences from *Arabidopsis* (*Ath*, archaebacterial-type, accession no. AF020715), *M. jannaschii* (*Mja*, accession no. Q58406), *E. coli* (*Eco*, accession no. P04804), rice cytosolic (*Osa*, accession no. Z85984), *S. cerevisiae* cytosolic/mitochondrial (*Sce*, accession no. P07263), and human cytosolic (*Hsa*, accession no. P12081). The numbering of the rice sequence tentatively starts from the same position as the *Arabidopsis* one, because the rice HisRS has a long putative N-terminal extension (data not shown). The three motifs that characterize class II aminoacyl-tRNA synthetases and the two HisRS-specific conserved blocks are underlined. Amino acids that are identical in three or more sequences are boxed.

no. R90550) probably represents a cDNA for cytosolic HisRS, because the deduced amino acid sequence is much more similar to cytosolic HisRSs from rice [15] and humans [16] (67% and 49% amino acid identity, respectively) than to *E. coli* HisRS (22% identity) [17]. The other type (exemplified by accession no. H36569) shares moderate sequence similarity rather equally with HisRSs from eukaryotes, prokaryotes, and archaebacteria (25–33% deduced amino acid identity), and thus was selected as a possible candidate for an organellar enzyme.

The complete sequencing of the clone revealed that it encodes a probable full-length cDNA of 1544 bp for a novel HisRS, termed AtHRS1. The deduced 486 amino acid sequence revealed extensive overall similarity with HisRS sequences from other organisms (Fig. 1). Surprisingly, the AtHRS1 amino acid sequence is most similar to HisRSs from archaebacterial counterparts, i.e. 33% amino acid identity with *Methanococcus jannaschii* HisRS (SwissProt accession no. Q58406) and 32% identity with *Methanobacterium thermoautotrophicum* HisRS (Genbank accession no. AE000811), respectively. In contrast, the AtHRS1 sequence displays less similarity to HisRSs from eukaryotes and prokaryotes, i.e. 31%, 30% and 28% amino acid identity with those from rice (cytosolic), *E. coli*, and human (cytosolic), respectively.

AtHRS1 contains all three conserved sequence motifs characteristic of class II aminoacyl-tRNA synthetases [1,2] as shown in Fig. 1. Furthermore, two sequence blocks conserved among known HisRSs [18] are clearly present in the AtHRS1 sequence, i.e. VVRGLAYY (residues 332–337), and GGRYDRL (residues 357–363). These blocks have been shown to form a histidine-binding pocket from the analysis of the three-dimensional structure of HisRSs from *E. coli* [19] and *T. thermophilus* [20].

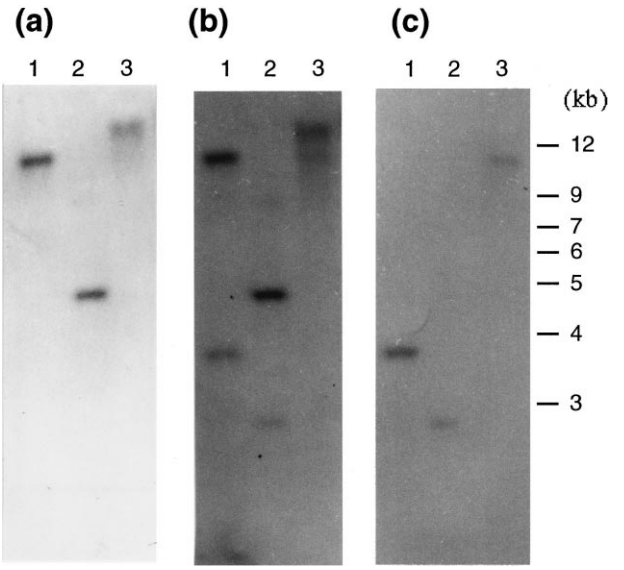

Fig. 2. Southern blot analysis. Genomic DNA (2 μg) of total *Arabidopsis* DNA was digested with restriction enzymes as indicated at the top of each lane. The filter was probed with random primed ^{32}P DNA probes derived from (a, b) the AtHRS1 cDNA, or (c) the 2nd EST clone T43519, respectively. Filters were washed under stringent conditions (30 min at 65°C in 0.1×SSC, 0.1% SDS) for a and c, or less stringent conditions (30 min at 51°C in the same buffer) for b, respectively.

The conservation of the motifs described above, together with the considerable sequence identity of AtHRS1 with HisRSs from other organisms, strongly suggest that this is a functional HisRS. The existence of the other EST clone (R90550) for cytosolic-type HisRS mentioned above indicated that AtHRS1 may function in a different subcellular compartment, i.e. mitochondria and/or chloroplasts. Consistent with this idea, the HisRS alignment revealed the presence of an N-terminal extension in AtHRS1 (Fig. 1), with a possible role in organelle targeting. AtHRS1 is 64 amino acids longer at the N-terminus than the *M. jannaschii* HisRS, and even 14 amino acids longer than the *S. cerevisiae* mitochondrial HisRS, which has a 20 amino acid mitochondrial presequence at its N-terminus [21]. The first 50 amino acids of AtHRS1 are enriched for leucine, serine and arginine residues, and contain only a single acidic residue. This biased composition is a common hallmark for mitochondrial and chloroplast targeting sequences [22]. The MitoProt II software [23] strongly predicts that the AtHRS1 presequence is a mitochondrial targeting sequence.

3.2. Two archaebacterial-like HisRS genes in Arabidopsis

To examine copy number of the archaebacterial-like HisRS gene in the *Arabidopsis* genome, we performed Southern blot analysis (Fig. 2) using the AtHRS1 cDNA as a probe. Under stringent washing conditions (calculated to reveal nucleotide sequences more than 94% identical to the probe), only single band was evident in each lane (Fig. 2a), corresponding to the gene encoding AtHRS1. However, when less stringent conditions were used (to reveal sequences with only 80% identity) with the same filter, an additional band was detected in each lane (Fig. 2b), suggesting another related gene in the *Arabidopsis* genome. In agreement with these observations, another EST sequence (Genbank accession no. T43519) has been reported recently from *Arabidopsis* that resembles the AtHRS1 cDNA. We confirmed by sequence analysis that the second EST clone corresponds to a partial cDNA including 318 nt of coding region with 89% nucleotide identity with the C-terminal portion of the AtHRS1 cDNA. A 13 nt deletion in a well-conserved region towards the C-terminus (corresponding to residues 461–464 in AtHRS1) results in a frame-shift of the final 25 codons of the cDNA. As this region of HisRS is thought to be involved in $tRNA^{His}$ binding [19], one can wonder whether this sequence encodes a functional HisRS. When the second EST clone, T43519, was used as a hybridization probe on the same filter, strong signals were observed in exactly the same positions as the weaker bands with the AtHRS1 cDNA probe (Fig. 2c), demonstrating that the second gene copy corresponds to this EST. We conclude that at least two archaebacterial-like HisRS sequences of more than 80% nucleotide identity are encoded in the *Arabidopsis* genome, although it is not yet apparent whether the second gene is functional.

3.3. Intracellular localization of AtHRS1 using a GFP fusion

To determine the cellular localization of the AtHRS1 product, a recombinant plasmid (termed AtHRS-GFP) was constructed in which the first 71 codons of the AtHRS1 cDNA, encoding the putative targeting peptide, were fused to the coding sequence of *Aequorea victoria* green fluorescent protein (GFP) [24]. As controls, we used fusion constructs encoding CoxIV-GFP [25] and RecA-GFP [26], in which the targeting

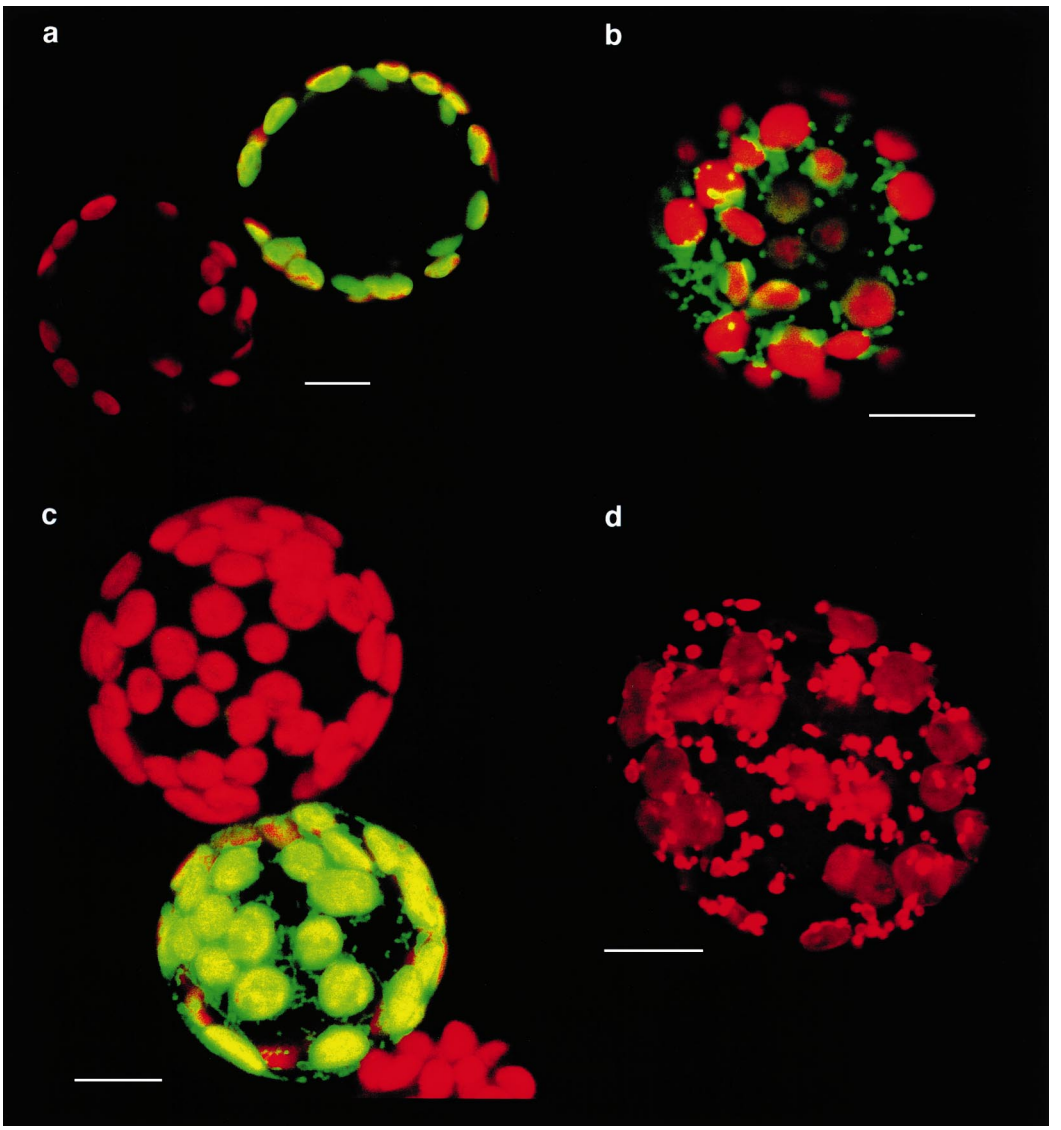

Fig. 3. Transient expression of GFP fusions in tobacco protoplasts. Cells expressing a: RecA-GFP fusion protein, b: CoxIV-GFP fusion protein, and c: AtHRS-GFP fusion protein are shown. d shows a protoplast stained with MitoTracker Red. The red channel (chloroplast fluorescence, and in d MitoTracker fluorescence) and the green channel (GFP) were collected separately as described in Section 2. c and d are maximum projections of about a dozen optical 'slices' through the upper half of the protoplasts. The scale bar is 10 μm in all images.

peptides from yeast mitochondrial CoxIV and *Arabidopsis* chloroplast RecA, respectively, were fused to GFP. It has already been established that these two fusion proteins are faithfully targeted to each organelle upon expression in plant cells [25,26].

When the RecA-GFP fusion construct was introduced into tobacco leaf protoplasts by electroporation and analyzed by confocal fluorescence microscopy, GFP fluorescence was localized exclusively in oval structures 3–6 μm in diameter, and perfectly matched with red autofluorescence from chloroplast pigments (Fig. 3a), demonstrating that this fusion protein is efficiently targeted to chloroplasts in this system. In cells expressing the CoxIV-GFP fusion protein, green fluorescence was observed in hundreds of round, oval or rod-like particles of 0.5–1 μm diameter, scattered throughout the cytoplasm (Fig. 3b), indicating that the CoxIV-GFP fusion proteins were efficiently delivered into mitochondria. A very similar pattern was obtained by staining protoplasts with the mitochondrial-specific dye MitoTracker Red (Fig. 3d). In cells expressing the AtHRS-GFP fusion protein, the GFP fluorescence was found to be localized in both mitochondria and chloroplasts (Fig. 3c). A low resolution double staining experiment using AtHRS-GFP and MitoTracker Red showed that the GFP fluorescence in mitochondria corresponded to the staining pattern seen with the dye, confirming the mitochondrial localization of the AtHRS-GFP fusion protein (data not shown).

The strength of the AtHRS-GFP signals in mitochondria and chloroplasts was somewhat lower than those of either of the organelle-specific controls. Supposing the level of expression is the same in these three fusion constructs, this may be partly due to dilution of the GFP because of the dual targeting. No background green fluorescence was detected in the cytosol or nucleus indicating the targeting was highly specific in all cases.

4. Discussion

4.1. Dual targeting

Previous work on organelle targeting has relied on difficult cell-fractionation experiments and in vitro import assays. The former approach suffers from recurring problems with cross-contamination of organelles, and the latter approach suffers in addition from the fact that import in vitro does not always faithfully reflect what happens in vivo (see for an example, [27]). The use of GFP fusions to investigate the function of presequences offers a rapid, technically simple and non-invasive technique to study targeting in vivo, and is ideal for analysing dual targeting, as although both chloroplasts and mitochondria are present in the system, allowing competition between them for the precursor protein, all problems associated with cross-contamination are avoided. Nevertheless, a number of potential difficulties need to be kept in mind. The first is the identification of the labelled organelles; although chloroplasts are easily recognized, other smaller organelles or vesicles can be confusing. Good quality high resolution images need to be obtained and compared to images showing GFP fusions of known localization in the same cell types. Organelle-specific dyes such as the MitoTracker used here are also useful, although they are not as specific as GFP fusion proteins. A second potential difficulty is an effect of the GFP moiety on the targeting activity of the fused presequence. This is difficult to completely rule out, but at least the RecA and CoxIV fusions demonstrate that GFP does not intrinsically hinder targeting to chloroplasts or mitochondria. To sum up, we are convinced that the HisRS-GFP fusion does enter both mitochondria and chloroplasts; this strongly implies, but does not prove, that AtHRS1 is also targeted to both organelles.

Dual targeting of a single gene product to both mitochondria and chloroplasts has been described previously, but many of the published cases result from heterologous expression, such as, for example, the plant or algal chloroplast transit peptides that can target proteins to fungal mitochondria [28,29] or the yeast mitochondrial targeting sequence that can address a passenger protein to both chloroplasts and mitochondria in plant cells [30]. Only a few natural examples are known, namely glutathione reductase [31], ferrochelatase-I [32] and methionyl-tRNA synthetase [33]. The manner by which dual targeting is achieved is not yet clear, but it is apparent from the experiments described here that the targeting information for both organelles resides in the same presequence. Attempts to present chloroplast and mitochondrial targeting sequences in tandem showed that the most N-terminal sequence is dominant, internal sequences being ineffective [34]. Hence it is likely that dual targeting is achieved because the presequence is 'ambiguous', and the same sequence is recognized by the import machinery in both chloroplasts and mitochondria, rather than because the presequence contains two independent targeting signals. This is interesting, because our current knowledge of plant mitochondrial and chloroplast protein import has uncovered no common factors (other than perhaps some cytosolic chaperones needed for unfolding the polypeptide before import), and the outer membrane receptors responsible for binding the presequence are thought to be different in the two organelles (for a review, see [35]). Nevertheless, the respective targeting peptides do show some similarities; in particular, both are generally positively charged, lack acidic residues, and are rich in alanine, leucine and hydroxylated amino acids. In amino acid composition, the AtHRS1 presequence generally fits expectations for both chloroplast and mitochondrial presequences. Like chloroplast transit peptides it is particularly rich in serine, but unlike them it does not contain the usual alanine following the initial methionine. Instead, there is an arginine, which is quite frequent in mitochondrial targeting peptides but unusual in chloroplast ones, which tend to lack charged amino acids at the N-terminus. Concerning potential cleavage sites, there are matches in the primary sequence to the proposed consensus sites for cleavage by both mitochondrial and chloroplast processing enzymes (RQFS, amino acids 31–34, which by the R-10 rule for mitochondrial processing [36] predicts cleavage between amino acids 40 and 41 and ICAA, amino acids 40–43, for stromal processing [37], predicting cleavage between amino acids 42 and 43).

4.2. Functional and evolutionary implications

The results presented here strongly imply that the *Arabidopsis* mitochondrial and plastid HisRSs are identical. This is not that surprising, because the mitochondrial $tRNA^{His}$ in *Arabi-*

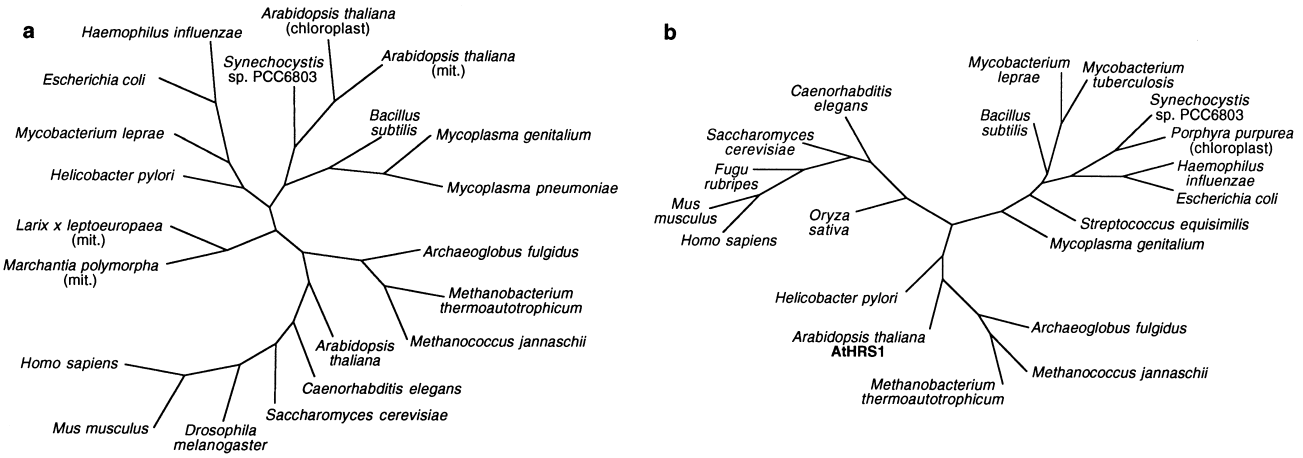

Fig. 4. Phylogenetic trees of a: $tRNA^{His}$ and b: HisRS sequences. The lengths of the internal branches are proportional to the frequency with which they were found in bootstrap replicates. See Section 2 for more detail. The tree topologies were supported by several methods of tree construction (parsimony methods, maximum likelihood methods, and distance matrix methods). mit., mitochondrial.

dopsis and other dicot plants is derived from a gene transferred from plastid DNA [10]. Hence, the chloroplast and mitochondrial $tRNAs^{His}$ are extremely similar. A similar situation is found for the mitochondrial and chloroplast $tRNA^{Met}$ and MetRS [33]. The question which arises immediately is the origin of this dual-targeted HisRS. The most natural assumption would be that it derives from the ancestor of the present-day chloroplasts, as it is clear that this is the origin of its tRNA substrate (Fig. 4a). *Synechocystis* is the organism most closely resembling the putative plastid ancestor for which much sequence data are available, but database searches and pairwise comparisons with other HisRSs suggest that AtHRS1 is more closely related to HisRSs from archaebacteria than to those from eukaryotes and prokaryotes, including *Synechocystis*. To evaluate these relationships in more detail, phylogenetic trees were constructed using HisRS sequences from various organisms (Fig. 4b). AtHRS1 clusters with archaeal HisRSs, but the association is not robust. There is clearly no close relationship with the HisRSs from *Synechocystis* or the chloroplast-encoded HisRS of the red alga *Porphyra purpurea*, showing that AtHRS1 is not derived from the original plastid gene. However, it is noteworthy that *Helicobacter pylori* HisRS is situated in a similar phylogenetic position to AtHRS1. *H. pylori* is classified in the δ/ε subdivision of the proteobacteria, whereas *H. influenzae* and *E. coli* are in the γ subdivision, and the probable mitochondrial ancestor is thought to be derived from the α subdivision [38]. Whole genome sequencing of *H. pylori* has revealed that nearly all its aaRS genes are similar to those of *E. coli* and *H. influenzae*, but HisRS was singled out as an exception [39]. It would be an incredible coincidence if the HisRSs of both *H. pylori* and plant organelles were derived by horizontal gene transfer from an unknown archaebacteria, and thus the best explanation appears to be that these sequences resemble the original proteobacterial HisRS (in which case the plant organellar enzyme is derived from the mitochondrial ancestor). This in turn implies that the HisRS sequences in *E. coli* and *H. influenzae* have evolved very rapidly away from their proteobacterial counterparts or that a common ancestor of the two acquired a HisRS gene from a non-proteobacterial eubacteria.

According to this evolutionary scenario, successful gene transfer of the HisRS gene from the ancestral mitochondrial DNA to the nucleus would have been followed by modification of its N-terminal targeting sequence to allow dual targeting to both mitochondria and chloroplasts, resulting in the functional replacement of the original chloroplast HisRS. It would be interesting to know whether or not the dual targeting preceded the transfer of the plastid $tRNA^{His}$ gene to mitochondrial DNA; such studies are possible, as some plants still contain a bona fide native mitochondrial $tRNA^{His}$ [40].

Acknowledgements: This work was supported by a grant from the JSPS to K.A.

References

[1] Eriani, G., Delarue, M., Poch, O., Gangloff, J. and Moras, D. (1990) Nature 347, 203–206.
[2] Moras, D. (1992) Trends Biochem. Sci. 17, 159–164.
[3] Shiba, K., Motegi, H. and Schimmel, P. (1997) Trends Biochem. Sci. 22, 453–457.
[4] Shiba, K., Suzuki, N., Shigesada, K., Namba, Y., Schimmel, P. and Noda, T. (1994) Proc. Natl. Acad. Sci. USA 91, 7435–7439.
[5] Shiba, K., Schimmel, P., Motegi, H. and Noda, T. (1994) J. Biol. Chem. 269, 30049–30055.
[6] Steinmetz, A. and Weil, J.H. (1986) Methods Enzymol. 118, 212–231.
[7] Maréchal-Drouard, L., Weil, J.H. and Dietrich, A. (1993) Annu. Rev. Plant Physiol. Plant Mol. Biol. 44, 13–32.
[8] Mireau, H., Lancelin, D. and Small, I.D. (1996) Plant Cell 8, 1027–1039.
[9] Dietrich, A., Maréchal-Drouard, L., Carneiro, V., Cosset, A. and Small, I. (1996) Plant J. 10, 913–918.
[10] Unseld, M., Marienfeld, J.R., Brandt, P. and Brennicke, A. (1997) Nature Genet. 15, 57–61.
[11] Ausubel, F.M., Brent, R., Kingston, R.E., Moore, D.D., Seidman, J.G., Smith, J.A. and Struhl, K. (1990) John Wiley and Sons, New York.
[12] Reichel, C., Mathur, J., Eckes, P., Langenkemper, K., Koncz, C., Schell, J., Reiss, B. and Maas, C. (1996) Proc. Natl. Acad. Sci. USA 93, 5888–5893.
[13] Carneiro, V.T.C., Pelletier, G. and Small, I. (1993) Plant Mol. Biol. 22, 681–690.
[14] Newman, T. et al. (1994) Plant Physiol. 106, 1241–1255.
[15] Akashi, K. and Small, I.D. (1997) Plant Physiol. 113, 1464.
[16] Raben, N., Borriello, F., Amin, J., Horwitz, R., Fraser, D. and Plotz, P. (1992) Nucleic Acids Res. 20, 1075–1081.
[17] Freedman, R., Gibson, B., Donovan, D., Biemann, K., Eisenbeis, S., Parker, J. and Schimmel, P. (1985) J. Biol. Chem. 260, 10063–10068.
[18] Menguito, C.A., Keherly, M.J., Tang, C., Papaconstantinou, J. and Weigel, P.H. (1993) Nucleic Acids Res. 21, 615–620.
[19] Arnez, J.G., Harris, D.C., Mitschler, A., Rees, B., Francklyn, C.S. and Moras, D. (1995) EMBO J. 14, 4143–4155.
[20] Aberg, A., Yaremchuk, A., Tukalo, M., Rasmussen, B. and Cusack, S. (1997) Biochemistry 36, 3084–3094.
[21] Natsoulis, G., Hilger, F. and Fink, G.R. (1986) Cell 46, 235–243.
[22] von Heijne, G., Steppuhn, J. and Herrmann, R. (1989) Eur. J. Biochem. 180, 535–545.
[23] Claros, M.G. and Vincens, P. (1996) Eur. J. Biochem. 241, 779–786.
[24] Chalfie, M., Tu, Y., Euskirchen, G., Ward, W.W. and Prasher, D.C. (1994) Science 263, 802–805.
[25] Kohler, R.H., Zipfel, W.R., Webb, W.W. and Hanson, M.R. (1997) Plant J. 11, 613–621.
[26] Kohler, R.H., Cao, J., Zipfel, W.R., Webb, W.W. and Hanson, M.R. (1997) Science 276, 2039–2042.
[27] de Castro Silva-Filho, M., Wieers, M.C., Flugge, U.I., Chaumont, F. and Boutry, M. (1997) J. Biol. Chem. 272, 15264–15269.
[28] Brink, S., Flugge, U.I., Chaumont, F., Boutry, M., Emmermann, M., Schmitz, U., Becker, K. and Pfanner, N. (1994) J. Biol. Chem. 269, 16478–16485.
[29] Hurt, E.C., Soltanifar, N., Goldschmidt-Clermont, M., Rochaix, J.-D. and Schatz, G. (1986) EMBO J. 5, 1343–1350.
[30] Huang, J., Hack, E., Thornburg, R.W. and Myers, A.M. (1990) Plant Cell 2, 1249–1260.
[31] Creissen, G., Reynolds, H., Xue, Y. and Mullineaux, P. (1995) Plant J. 8, 167–175.
[32] Chow, K.S., Singh, D.P., Roper, J.M. and Smith, A.G. (1997) J. Biol. Chem. 272, 27565–27571.
[33] Menand, B., Maréchal-Drouard, L., Sakamoto, W., Dietrich, A. and Wintz, H. (1998) Proc. Natl. Acad. Sci. USA, in press.
[34] de Castro Silva Filho, M., Chaumont, F., Leterme, S. and Boutry, M. (1996) Plant Mol. Biol. 30, 769–780.
[35] Heins, L., Collinson, I. and Soll, J. (1998) Trends Plant Sci. 3, 56–61.
[36] Gavel, Y. and von Heijne, G. (1990) Protein Eng. 4, 33–37.
[37] Gavel, Y. and von Heijne, G. (1990) FEBS Lett. 261, 455–458.
[38] Leblanc, C., Richard, O., Kloareg, B., Viehmann, S., Zetsche, K. and Boyen, C. (1997) Curr. Genet. 31, 193–207.
[39] Tomb, J.F. et al. (1997) Nature 388, 539–547.
[40] Maréchal-Drouard, L., Kumar, R., Remacle, C. and Small, I. (1996) Nucleic Acids Res. 24, 3229–3234.